



3D Printing and Adenosine Receptor Activation for Craniomaxillofacial Regeneration

Christopher D. Lopez, Lukasz Witek,
Roberto L. Flores, Andrea Torroni,
Eduardo D. Rodriguez, Bruce N. Cronstein,
and Paulo G. Coelho

18.1 Background

Maxillofacial reconstruction has evolved over the past 15 years toward customized treatment plans which fulfill both functional and aesthetic outcomes of facial restoration. The merger of cranio-maxillofacial and microvascular principles has given rise to tailored-specific free tissue flaps which reconstruct bony maxillofacial defects while rebuilding lining, soft tissue mass, and

facial subunits—all of which are key to achieving outcomes that approach normalcy. In addition, surgical planning technology has been able to expedite functional recovery: flap-based reconstruction of the mandible and maxilla with pre-planned dental prosthesis can be completed in one operation instead of requiring rehabilitation periods that can take up to a year [1, 2].

While only a small subset of facial trauma requires free tissue transfer, the severity of these cases has been the impetus for the recent advances in craniomaxillofacial and microvascular principles. Unfortunately, the contemporary techniques for complex maxillofacial reconstruction remain limited: autologous bone transfer is complicated by limited bone stock and shape, donor site morbidity, surgical site infection, delayed healing, long operative times, and cost [3, 4]. In appreciation of these limitations, advances in bone tissue engineering have sought to restore maxillofacial deficiencies using customizable constructs commonly augmented with osteogenic agents and/or cellular therapy. The numerous bone constructs described, coupled with the paucity of clinically available tissue engineering-based therapies, highlight the importance of highly translational approaches that consider the challenges faced when attempting bench-to-bedside deployment.

C. D. Lopez · P. G. Coelho (✉)
Hansjörg Wyss Department of Plastic Surgery, NYU
Langone Health, New York, NY, USA

Department of Biomaterials and Biomimetics, NYU
College of Dentistry, New York, NY, USA
e-mail: christopher.lopez2@nyumc.org; Pc92@nyu.edu

L. Witek
Department of Biomaterials and Biomimetics, NYU
College of Dentistry, New York, NY, USA
e-mail: Lw901@nyu.edu

R. L. Flores · A. Torroni · E. D. Rodriguez
Hansjörg Wyss Department of Plastic Surgery, NYU
Langone Health, New York, NY, USA
e-mail: Roberto.Flores2@nyumc.org; Andrea.Torroni@nyumc.org; Eduardo.rodriguez@nyumc.org

B. N. Cronstein
Department of Medicine, NYU Langone Health,
New York, NY, USA
e-mail: Bruce.cronstein@nyumc.org

In this chapter, we will review recent developments our laboratory has made in materials science, osteogenic stimulation, and the integration of these components into an informed tissue engineering construct for maxillofacial bony restoration.

18.2 Advances in Material Science

Calcium phosphate-based biomaterials have been used clinically for decades and have well-established biocompatibility and safety properties [5, 6]. As a result, these biomaterials are used as bone graft substitutes in over half of all grafting procedures in the United States annually [7]. While outcomes are generally favorable for small-scale bony defects, large defects require an interface between the implant and bone margin that facilitates osteoconduction and implant absorption. This is not possible with granular or en bloc materials which are easily manufactured in high quantities and, consequently, cannot be customized to address unique anatomic defects in a personalized fashion. Additionally, they lack both the geometric stability, spatial coordination, and degradation kinetics necessary to maximize bone formation through osteogenesis and osseoconduction.

18.2.1 Geometric Considerations and the Role of 3D Printing in Scaffold Design

The concept that geometric design of biomaterials can alter bone healing is relatively new. Over

the last decade, reports investigating bone healing in endosteal metallic implants have determined that osseoconduction is dependent on many physicochemical factors that can be manipulated. This includes macrogeometric-, micrometer-, and nanometer-level changes in implantable device physical dimensions as well as its relationship to the osteotomy walls created by surgical instrumentation [8–11]. These analyses of implant geometry have elucidated that early and late stages of bone healing are directly related to implantable device design and can be leveraged to maximize bone formation. More recently, these principles have seen successful translation to other biomaterials that are even more suited to facilitate bone formation: calcium phosphate-based bioactive ceramics [5, 12–14].

Although calcium phosphate-based bio-ceramics typically exist in powder form, the advent of biomedical applications for 3D printing has yielded modalities capable of printing these bio-ceramics as an ink/slurry capable of holding form. As a result, 3D printing has become a powerful tool capable of printing calcium phosphate-based bio-ceramics in any form, making it a tool of significant interest to tissue engineering and surgery communities.

Three-dimensional printing can create a personalized scaffold macrogeometry based on clinical imaging and thus offers a valuable approach to patient-specific bony defects. By using computer-aided design and manufacturing (CAD/CAM), scaffold constructs can be designed to any bulk shape and size as well as a porous design (Fig. 18.1a–c). Despite the existence of 3D printing for biomedical applications for over a decade, bone

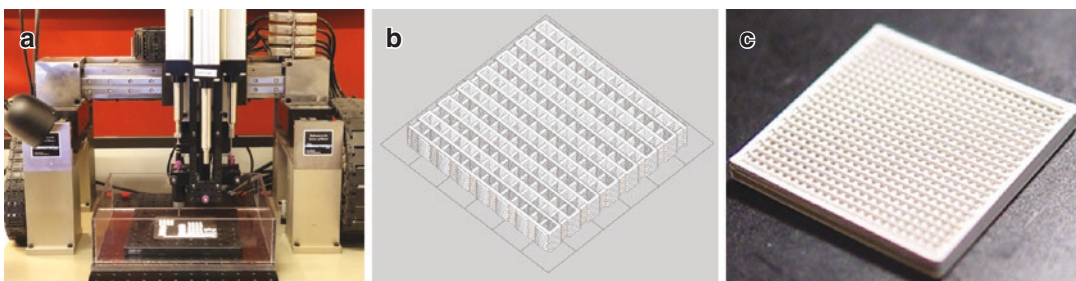


Fig. 18.1 3D printing. (a) Printer, (b) CAD/CAM software design of scaffold, and (c) scaffold after printing

regeneration using 3D printing has remained mixed in outcomes until recently [15–29]. It is suggested that these results are consequent to approaches to 3D printing that do not take advantage of the lessons learned from endosteal implant bone healing. A review of factors that affect bone healing in metallic biomaterials clearly cites that dimensions ranging from macrogeometric to nanogeometric all merit consideration. Only recently have these dimensions been investigated through 3D printing [5, 9] in a stepwise fashion.

18.2.2 β -Tricalcium Phosphate

Historically, the investigation of bio-ceramics for bone healing has been predominantly focused on hydroxyapatite (HA). HA is the main inorganic component of the bone, making its study a logical choice. Furthermore, HA has favorable bone regenerative properties such as biocompatibility and osseointegration. However, it also has less desirable properties, such as unfavorable resorption kinetics. When designing scaffolds for bone regeneration, an ideal construct should ideally facilitate bone formation at a defect and then resorb/degrade without operative intervention. Unfortunately, HA has a low resorption rate in vivo of approximately 1–2% per year at 5 years post-implantation [30], thereby limiting complete bony regeneration.

β -Tricalcium phosphate (β -TCP), on the other hand, has far more rapid resorption/degradation kinetics both in vitro and in vivo when compared to HA. A biomaterial that is also highly osseointegrative and biocompatible, β -TCP can facilitate bone regeneration while also demonstrating favorable resorption that happens in tandem with bone formation. This unique material property can be manipulated to a significant degree with modalities such as 3D printing: when designing scaffold interstices, the rate of degradation can be altered by mesogeometric changes in lattice porosity size, strut circumference, or any other change that alters the surface area. At the nanogeometric level, alterations in ink formulation or sintering that alter porosity can also be engineered to tailor the scaffold degradation rate.

18.3 Bioactive Molecules

18.3.1 Adenosine Receptors

A wide array of biologic agents have been investigated in order to alter bone metabolism in favor of bone formation/healing. Of note, the recently described purinergic receptors have demonstrated promising bone regenerative potential [13, 31–35].

Adenosine has been termed the “retaliatory metabolite” for its unique physiologic role: it is secreted in response to ATP depletion, serves as a marker of metabolic status at the cellular level, and is known to attenuate activity for a wide array of cell types as a protective mechanism. For example, unstressed tissues have an extracellular adenosine concentration of $\sim 1 \mu\text{M/L}$, but in septic patients, this number can increase tenfold [36]. When released, adenosine binds to receptors on the surface of immune cells and regulates exuberant immune responses. A practical example is adenosine binding to receptors on neutrophils and inducing the suppression of superoxide anion [37]. These regulatory effects have been reported for almost a century: Drury and Szent-Gyorgyi reported in 1929 that adenosine induced a protective vasodilatory and negative inotropic effect on stressed cardiac vessels and tissue. Today, this mechanism is taken advantage of for cardiac stress testing.

Adenosine bioavailability is determined by regulated, interdependent cellular processes [38]. For example, in the setting of tissue hypoxia/ischemia, purinergic metabolic pathways increase dephosphorylation of ATP to adenosine inside the cell via 5' nucleotidase and suppress adenosine kinase activity, the enzyme needed to rephosphorylate adenosine [38]. Extracellular adenosine accumulates by two suggested mechanisms: the first involves precursor nucleotides (e.g., ATP, ADP, AMP) released from cells and catabolized into adenosine by several ectonucleosidases. The latter involves intracellular adenosine being shunted extracellularly by specialized nucleoside transporters [38].

There are four adenosine receptors: A1, A2A, A2B, and A3. A1 and A3 receptors are coupled to either Gi-coupled signal transduction proteins or

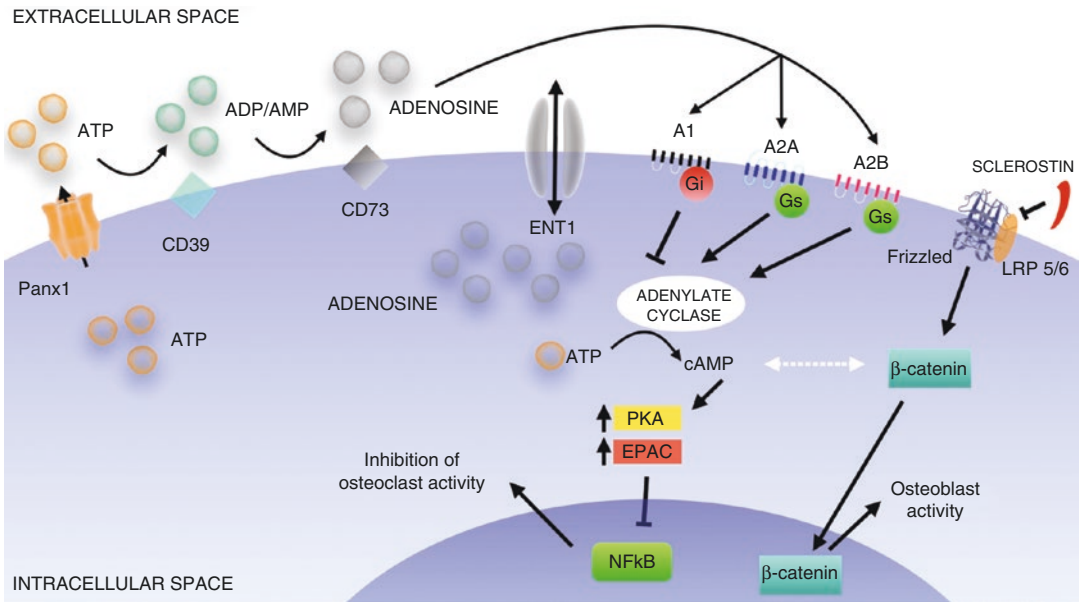


Fig. 18.2 Illustration of adenosine receptor intracellular pathway

ion channels, and A2 receptors are G-alpha-s-linked receptors that stimulate adenylyl cyclase/cAMP [39]. Adenosine receptors have effects on both osteoblast and osteoclast syntheses (Fig. 18.2) [40]. In brief, the following have been reported:

1. A1R ligation plays a role in osteoclast formation: In its absence or antagonism, defects have been reported to arise in CSF-1 (colony-stimulating factor 1) and RANK-L (receptor activator of nuclear factor κ -B ligand), thus A1R activation induces osteoclastogenesis both in vitro and in vivo [41].
2. A2AR activation inhibits osteoclastogenesis and A2AR antagonism activates it [42]. Also, osteoblast function is positively modulated by A2AR activation [43]. A2ARs seem to play a role in establishing osteoblast maturation and the maintenance of osteoblast phenotype [44]. A2AR gene and protein expression is upregulated at later stages of osteoblast differentiation [44] but is less present at earlier stages (e.g., undifferentiated stages of mesenchymal stem cells)—Furthermore, A2AR ligation does not alter the gene expression of markers of bone formation, such as *RUNX-2* or *ALP* at earlier stages, but it does upregulate osteogenesis at later stages of differentiation [44].
3. A2BR activation likely plays the most prevalent role in human primary osteoblast-like cells. Osteogenic differentiation seems to be most dramatic under the influence of A2B agonism [45], and it has been suggested that the significance of A2BRs lies in establishing commitment and differentiation of stem cells toward osteoblast lineage. A2BRs are the predominant adenosine receptor subtype expressed in undifferentiated mesenchymal stem cells (MSCs) and upon activation promote osteoblast lineage marker upregulation, osteoblastogenesis, and increases in mineralization.
4. A3AR has not been shown to directly affect osteoclastogenesis or osteoblast bone deposition when stimulated or blocked. However, A3 agonism has been shown to downregulate bone resorption and the number of osteoclasts in murine arthritis [46].

It is critical to note that the adenosine receptor-derived changes in bone homeostasis only occur at supraphysiologic concentrations [45]. Non-stressed cellular environments do not accumulate sufficient adenosine extracellularly to activate any of the aforementioned receptors—even with continuous blockage of the adenosine deaminase enzyme.

These supraphysiologic concentrations can be achieved with pharmacologic agents. An example that has garnered significant interest is dipyridamole, because of its well-established, decades-long safe clinical use in cardiac stress testing and antiplatelet therapy, even in pediatric patient populations [47–49]. Dipyridamole blocks adenosine uptake into the cell via type 1 equilibrative nucleoside transporter (ENT1) and thereby ensures extracellular accumulation.

18.4 The Integration of Tissue Engineering Principles

The bone regenerative capacity of adenosine receptor ligation is ideally leveraged via delivery to defect sites while avoiding systemic effects. This principle of localized drug delivery directly to injury sites is critical in order to avoid unintended effects resulting from activation of other systems—a likely event given the prevalent expression of the adenosine receptor. Furthermore, local delivery simplifies release kinetics and circumvents issues such as patient compliance with medication. Finally, the concentration of dipyridamole needed to affect alterations of bone metabolism is much lower when delivered locally as opposed to systemically, and this local delivery dosage is much lower than systemic concentrations already approved for adult and pediatric patients. Therefore, the local delivery model of dipyridamole may be well suited for future clinical deployment in conjunction with a bone tissue engineering scaffold.

A small but growing body of work demonstrates the effects of localized adenosine receptor activation via 3D-printed, geometrically tailored osseoconductive scaffold carriers.

18.4.1 Calvarial Defect Regeneration: Translation Between Species

The earliest *in vivo* report of localized adenosine receptor delivery for bone healing was by Mediero and colleagues in 2015. A collagen sponge replaced a murine calvarial defect, and it

was found that daily administration of dipyridamole regenerated the bone as well as BMP-2 [34]. Although these sponges supported bioactive molecule effects, they lacked the structural support necessary to fit and fill large bony defects and facilitate cellular communication and did not contribute regenerative properties alone. As a result, dipyridamole was more recently combined with 3D-printed bio-ceramic scaffolds which independently demonstrated osseoconductive properties and could be customized to geometrically restore any bony defect. A2A receptor activation was determined to be a critical mechanism of action for bone: in these same murine models, A2A receptor knockouts failed to regenerate cranial bone defects, while controls healed well, highlighting the critical role the A2A receptor plays in bone regeneration [50].

These same principles were also successfully demonstrated in even larger, more translational models: the sheep calvaria. The sheep had two ipsilateral trephine-induced (11-mm-diameter) calvarial defects at $t = 0$, and a second pair of trephines induced contralateral at $t = 3$ weeks. Scaffolds were coated in either 100 μM dipyridamole and a collagen carrier bound to the scaffold via cross-linking or the collagen carrier alone. Each side received one of each scaffold. Following euthanization for two end points ($t = 3$ weeks and $t = 6$ weeks), scaffolds were evaluated through micro-CT and non-decalcified histology. Both uncoated and dipyridamole-coated scaffolds exhibited regenerative properties, but dipyridamole significantly augmented this healing at both time points. Interestingly, A2AR activation seemed to have recruited the intrinsic osteogenic capacity of the local dura mater [13]. This capacity was previously observed by others [51].

18.4.2 Load-Bearing Translational Preclinical Models

The regenerative capacity of uncoated bio-ceramic scaffolds with deliberate geometric design has been demonstrated. Full-thickness, unilateral mandibulectomies ~12 mm in length

(compared to 10 mm partial-thickness defects qualifying as critical-sized) were performed on adult New Zealand white rabbits at the segmental mandibular body and replaced with 3D-printed scaffolds that replaced the defect in size and shape (Fig. 18.3a). At 8 weeks in vivo, β -tricalcium phosphate scaffolds demonstrated bone regeneration on gross examination (Fig. 18.3b). This significant degree of osseointegration bridged the defect span through initial extensive woven bone formation despite immediate return to masticatory function. Micro-CT imaging confirmed significant amounts of bone growth, and histology confirmed that at 8 weeks, intramembranous-like healing pathways are involved, depicting highly cellular, vascularized woven bone structure directly in contact with scaffold struts and lumen (Fig. 18.4a–c). Higher magnification imaging depicts resorbing scaffold along with areas of lamellar bone formation around primary osteonic structures. Electron microscopy illustrates intramembranous-like healing with entire woven to lamellar reorganization spectrum, scaffold resorption (Fig. 18.5), and formation of concentric rings. Microcracks that correspond to bone remodeling are also seen.

These 3D-printed scaffolds have also demonstrated regenerative capacity, both with and without dipyrindamole coating, at another part of the rabbit mandible: the load-bearing, relatively avas-

cular ramus. Critical-sized, full-thickness partial mandibulectomies of NZWR rami were performed and replaced with one of the three scaffold types: uncoated, 100 μ M dipyrindamole carried via collagen cross-linking to scaffold, and collagen carrier alone. Like the segmental body scaffold, these scaffolds were designed to precisely fit and fill the defect made (Fig. 18.6). At a point of $t = 8$ weeks, bone regeneration was markedly enhanced with the addition of dipyrindamole at the ramus, though all uncoated scaffolds and collagen-coated scaffolds did have bone growth with remodeling sites, vascular supply, and both immature woven bone and reorganized lamellar bone (Fig. 18.7). Scaffold degradation was also most extensive with dipyrindamole coating, likely because of the rebounding effects after the transient changes dipyrindamole has on the bone. Since normal bone homeostasis must eventually be reestablished, the effects of A2AR activation on osteoclast activity attenuation is likely followed by an increase in activity once dipyrindamole concentrations become too low to affect bone metabolism [34]. Of note, while collagen coating functions to carry dipyrindamole, collagen alone seems to limit the early stages of bone remodeling. It is likely that collagen impedes cellular communication between osteogenic cells that induce regeneration and the highly osseointegrative scaffold material. It has also been observed

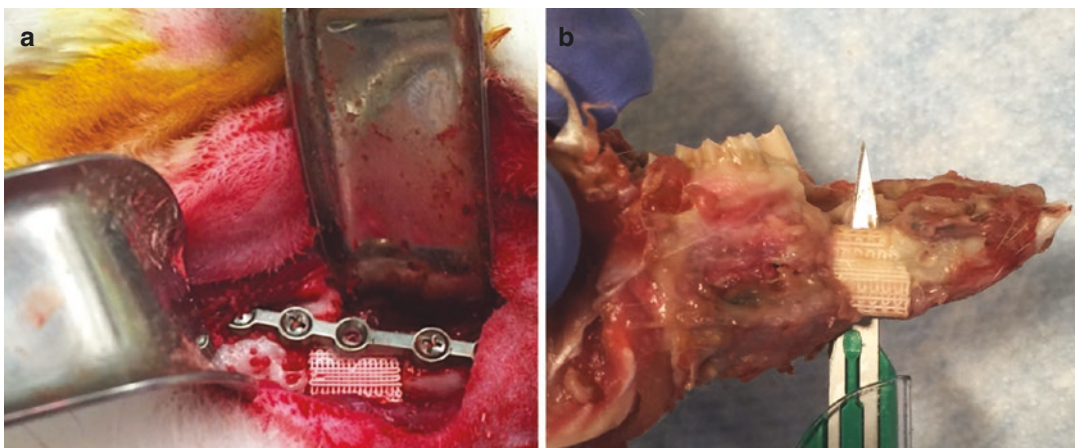


Fig. 18.3 (a) Intraoperative scaffold placement with plating for support and (b) scaffold integration with rabbit mandible at $t = 8$ weeks after necropsy



Fig. 18.4 (a) Sagittal histologic slice of scaffold in continuity with rabbit mandible. (b) High magnification from (a) demonstrating porous ingrowth. (c) Highly cellular

and vascularized woven bone structure, as well as newer, organized lamellar bone formation depicted by arrows (*I* Incisor, *T* tooth, *IAN* inferior alveolar nerve)

that dipyridamole actually facilitates a different pattern of healing than uncoated or collagen-coated scaffolds at the ramus: while it is expected that partial ramus mandibulectomies have the greatest regenerative potential at sites closest in proximity to three-wall defects, only dipyridamole-coated scaffolds demonstrated this healing pattern. Without dipyridamole, uncoated scaffolds and collagen-coated scaffold induced bone formation in uncoordinated pockets.

18.4.3 Skeletally Immature Translational Models

The challenges for regenerating the skeletally immature bone are different than that of a skeletally mature bone. Alveolar cleft defects of the

primary palate create structural instability of the maxillary arch, an inability to support tooth eruption, and facial asymmetry. Furthermore, current tissue engineering-based therapies must consider the growing maxillofacial skeleton and therefore cannot introduce therapies that will potentially induce premature suture fusion.

Skeletally immature NZWRs underwent unilateral, ~ 3.5 mm \times ~ 3.5 mm alveolar cleft defect injury visualized via a direct transfacial approach (Fig. 18.8a, b). Defects created without scaffold intervention served as negative controls, and scaffolds were coated with different concentrations of dipyridamole, 100, 1000, or 10,000 μ m, all carried by collagen cross-linked to scaffolds. After $t = 8$ weeks, animals were euthanized, and it was observed that the regenerative properties of 3D-printed scaffolds with dipyridamole induce

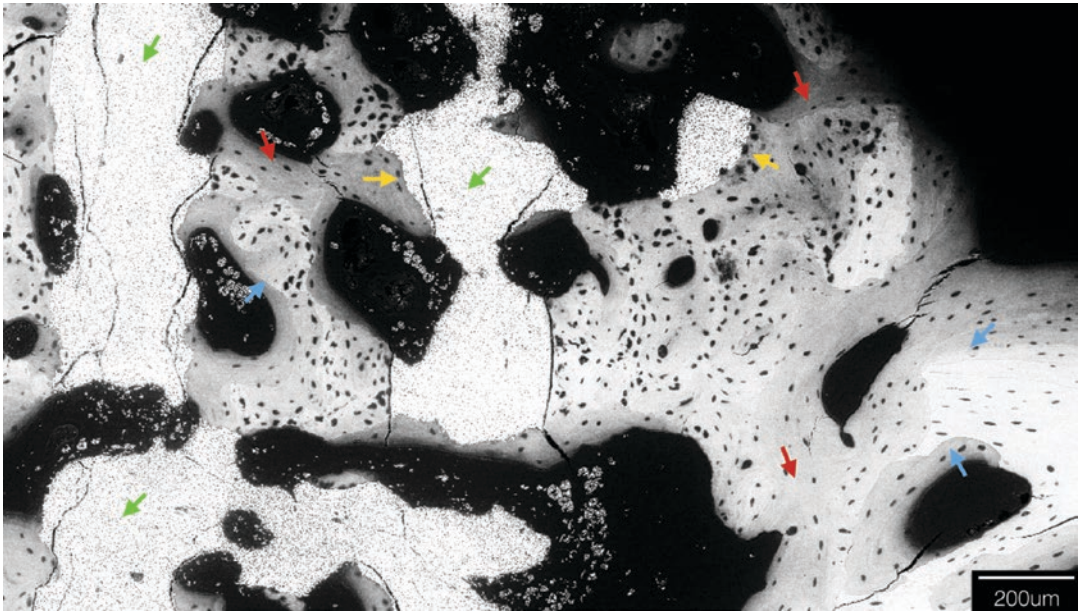


Fig. 18.5 Electron microscopy depicting scaffold struts (green arrows) and new, intramembranous like bone formation throughout scaffold interstices (red arrows). New, woven bone is seen filling sites of scaffold degradation

(yellow arrows), and regions of lamellar reorganization juxtaposed with immature woven bone are evident (blue arrows, lamellar as brighter bone, woven is darker)

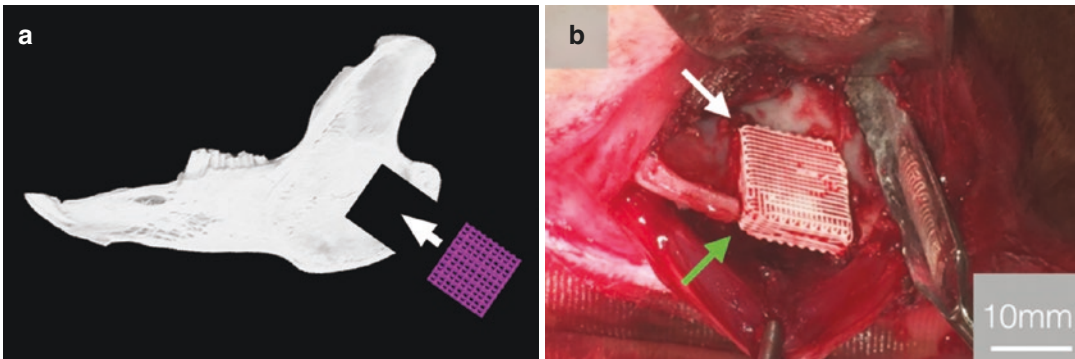


Fig. 18.6 (a) Surgical injury model depicting scaffold (purple) insertion site with arrow and (b) intra operative photo of scaffold placement at ramus

dose-dependent bone formation at the alveolar cleft in rabbits (Fig. 18.8c). Perhaps most importantly, even at doses of 1–2 logarithmic increases more than needed to increase bone formation, maxillary and sutures remained patent (Fig. 18.8c, d). Healing was both intramembranous-like and endochondral-like, with highly cellular and vascularized structure throughout scaffold porosity (Fig. 18.9).

18.5 Conclusions and Future Directions

The field of surgery arose from the need to visualize the treatment of disease, and its initial challenges were predominantly based on ensuring technical ability. Today's clinicians face a new challenge: the explosion of medical knowledge and innovation that continues to grow every day.

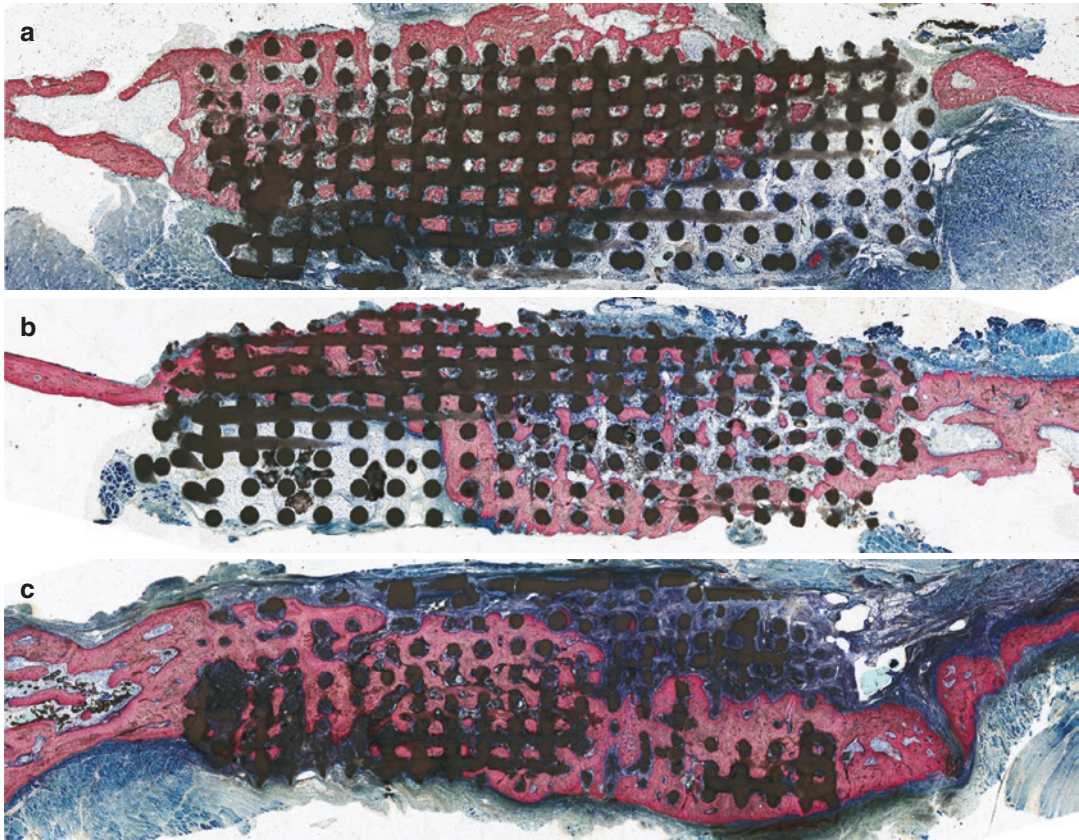


Fig. 18.7 Optical micrographs of scaffold inserted into ramus after 8 weeks. Bone (pink) on either side of scaffold depicts original ramus bone thickness and scaffold

(black) demonstrates directional bone growth throughout porosity. (a) Control group; (b) COLL group; (c) DIPY group

In a world where a plethora of biomaterials are readily available for reconstructive purposes, it is no longer sufficient to be a technically skilled surgeon. A strong understanding of regenerative materials available clinically, as well as those with significant translational potential, is essential for sound practice, surgical judgment, and innovative patient care. From linen sutures used in Ancient Egypt to custom, patient-specific 3D-printed bone-cutting guides used in facial transplantation today, biomaterials have a long, rich history in aiding human healing, and boundaries continue to be pushed.

Tissue engineering craniomaxillofacial bone has been the dream of reconstructive surgeons for over a quarter of a century. Unfortunately, early efforts yielded disappointing results of either limited volume or poor bone quality. The clinical

potential of tissue-engineered craniomaxillofacial regeneration has yet to be realized, but highly translational constructs are under active investigation. Three-dimensional printing bioactive ceramic scaffolds with deliberate geometries for osseointegration has provided regenerative cells with physical pathways to communicate with and fill defects by healing, and the porosity is also permissive to other variables that contribute to bone healing, such as blood clots rich in osteogenic factors [52]. For the first time, significant bone healing responses to load-bearing bones such as the body and ramus of the mandible are being reported. A2AR activation appears to stimulate local dura tissue to contribute to regeneration, and alveolar clefts respond to dipyridamole delivery in a dose-dependent manner without any changes to maxillary suture biology at 8 weeks.

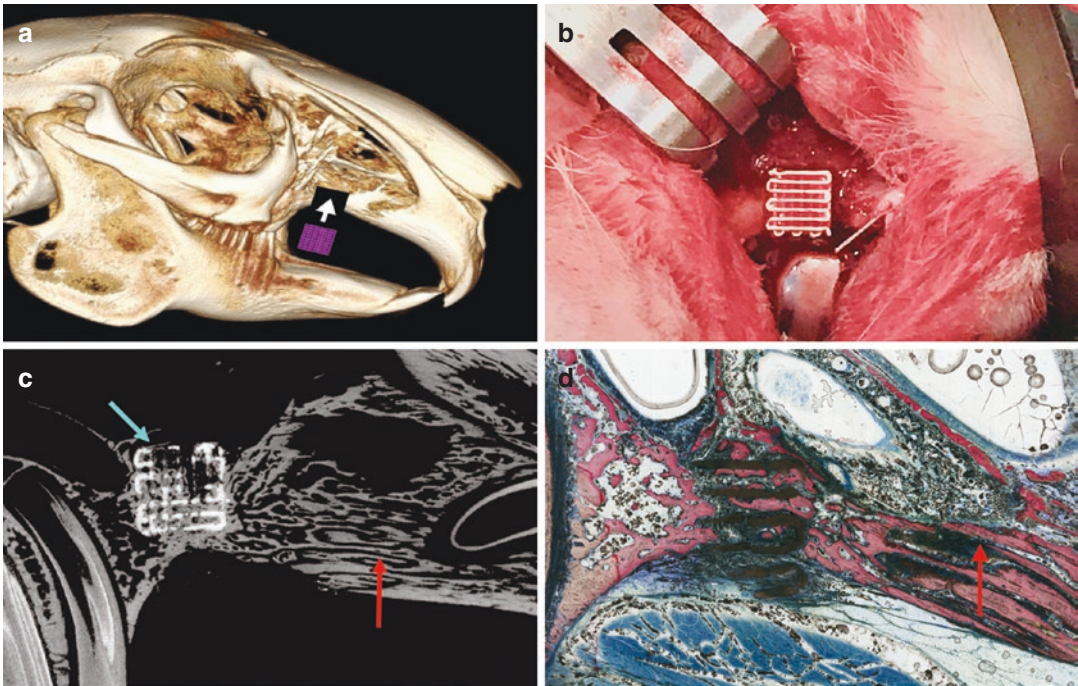


Fig. 18.8 Alveolar cleft model in immature rabbit maxilla at $t = 8$ weeks. (a) Schematic depicting surgical injury model with scaffold (purple) insertion site. (b) Intraoperative photo of scaffold insertion. (c) MicroCT

slice at $t = 8$ weeks with scaffold (blue arrow) and patent sutures (red arrow). (d) Non-decalcified histologic section of scaffold (black), new bone growth within scaffold (pink) and patent sutures (red arrow)

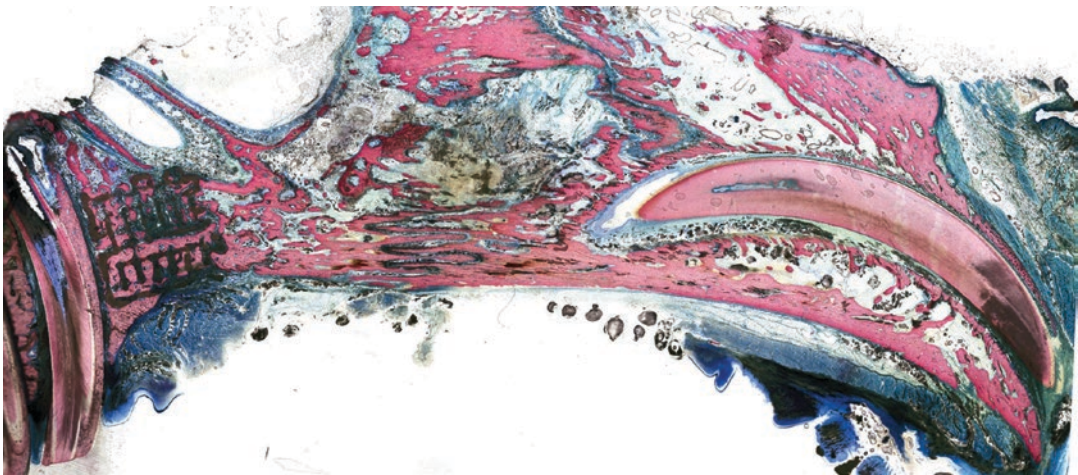


Fig. 18.9 Alveolar cleft with scaffold inserted and bone regeneration at $t = 8$ weeks. Scaffold (black) lattice with bone (pink) growth throughout porosity demonstrating

osseointegration via intramembranous and endochondral-like healing. Suture potency is noted as well in higher magnification (yellow arrow)

Favorable outcomes have been demonstrated by utilizing principles of biomaterial design alone, as well as with the addition of A2AR acti-

vation. While groups have also attempted to address the challenge of large bony defect regeneration through stem cell investigation and mol-

ecules such as bone morphogenetic proteins [53, 54], outcomes have been inconsistent. Unfortunately, clinical deployment of stem cell therapies has not yet demonstrated desired outcomes, and from a regulatory standpoint, they remain challenging to use and ethically debated. An approach to regeneration such as that presented in this chapter, with both biomaterials and bioactive molecules proven to be safe, which capitalize on endogenous healing mechanisms to work, has significant promise for clinical use and warrants further investigation.

Acknowledgments We would like to wholeheartedly thank Dr. Joseph G. McCarthy for his endorsement of our work and contributions to this chapter. His insight on advances and setbacks in craniomaxillofacial surgery over the last quarter of a century provides us with the unique opportunity to focus on clinically relevant challenges that have challenged reconstructive surgeons for decades.

The work presented in this chapter was supported by NIH/NIAMS 5R01AR068593-02, 3R01AR068593-02S1, 5R01AR068593-03, & 3R01AR068593-03S1, NIH/NICHD R21HD090664-01, and DoD W81XWH-16-1-0772. Drs. Coelho and Cronstein are co-inventors of the 3D printing technology presented in this chapter.

References

- Levine JP, Bae JS, Soares M, Brecht LE, Saadeh PB, Ceradini DJ, et al. Jaw in a day: total maxillofacial reconstruction using digital technology. *Plast Reconstr Surg.* 2013;131(6):1386–91.
- Runyan CM, Sharma V, Staffenberg DA, Levine JP, Brecht LE, Wexler LH, et al. Jaw in a day: state of the art in maxillary reconstruction. *J Craniofac Surg.* 2016;27(8):2101–4.
- Hidalgo DA. Condyle transplantation in free flap mandible reconstruction. *Plast Reconstr Surg.* 1994;93(4):770–81.
- Hidalgo DA, Rekow A. A review of 60 consecutive fibula free flap mandible reconstructions. *Plast Reconstr Surg.* 1995;96(3):585–96.
- Simon JL, Michna S, Lewis JA, Rekow DE, Thompson VP, Smay JE, et al. In vivo bone response to 3D periodic hydroxyapatite scaffolds assembled by direct ink writing. *J Biomed Mater Res A.* 2007;83A(3):747–58.
- Inzana JA, Olvera D, Fuller SM, Kelly JP, Graeve OA, Schwarz EM, et al. 3D printing of composite calcium phosphate and collagen scaffolds for bone regeneration. *Biomaterials.* 2014;35(13):4026–34.
- Roberts TT, Rosenbaum AJ. Bone grafts, bone substitutes and orthobiologics: the bridge between basic science and clinical advancements in fracture healing. *Organogenesis.* 2012;8(4):114–24.
- Steigenga JT, Al-Shammari KF, Nociti FH, Misch CE, Wang H-L. Dental implant design and its relationship to long-term implant success. *Implant Dent.* 2003;12(4):306–17.
- Wilson CE, de Bruijn JD, van Blitterswijk CA, Verbout AJ, Dhert WJA. Design and fabrication of standardized hydroxyapatite scaffolds with a defined macro-architecture by rapid prototyping for bone-tissue-engineering research. *J Biomed Mater Res A.* 2004;68A(1):123–32.
- Jimbo R, Anchietà R, Baldassarri M, Granato R, Marin C, Teixeira HS, Tovar N, Vandeweghe S, Janal MN, Coelho PG. Histomorphometry and bone mechanical property evolution around different implant systems at early healing stages: an experimental study in dogs. *Implant Dent.* 2013;22(6):596–603.
- Coelho PG, Jimbo R. Osseointegration of metallic devices: current trends based on implant hardware design. *Arch Biochem Biophys.* 2014;561:99–108.
- Ishack S, Mediero A, Wilder T, Ricci JL, Cronstein BN. Bone regeneration in critical bone defects using three-dimensionally printed β -tricalcium phosphate/hydroxyapatite scaffolds is enhanced by coating scaffolds with either dipyrindamole or BMP-2. *J Biomed Mater Res B Appl Biomater.* 2017;105(2):366–75.
- Bekisz JM, Flores RL, Witek L, Lopez CD, Runyan CM, Torroni A, et al. Dipyrindamole enhances osteogenesis of three-dimensionally printed bioactive ceramic scaffolds in calvarial defects. *J Craniomaxillofac Surg.* 2018;46(2):237–44.
- Lopez CD, Diaz-Siso JR, Witek L, Bekisz JM, Cronstein BN, Torroni A, et al. Three dimensionally printed bioactive ceramic scaffold osseointegration across critical-sized mandibular defects. *J Surg Res.* 2018;223:115–22.
- Seitz H, Rieder W, Irsen S, Leukers B, Tille C. Three-dimensional printing of porous ceramic scaffolds for bone tissue engineering. *J Biomed Mater Res B Appl Biomater.* 2005;74(2):782–8.
- Cai S, Xi J, Chua CK. A novel bone scaffold design approach based on shape function and all-hexahedral mesh refinement. *Methods Mol Biol.* 2012;868:45–55.
- Castilho M, Dias M, Gbureck U, Groll J, Fernandes P, Pires I, et al. Fabrication of computationally designed scaffolds by low temperature 3D printing. *Biofabrication.* 2013;5(3):035012.
- Wang X, Schröder HC, Müller WE. Enzymatically synthesized inorganic polymers as morphogenetically active bone scaffolds: application in regenerative medicine. *Int Rev Cell Mol Biol.* 2014;313:27–77.
- Zhou Z, Buchanan F, Mitchell C, Dunne N. Printability of calcium phosphate: calcium sulfate powders for the application of tissue engineered bone scaffolds using the 3D printing technique. *Mater Sci Eng C.* 2014;38:1–10.
- Farzadi A, Solati-Hashjin M, Asadi-Eydivand M, Osman NAA. Effect of layer thickness and printing

- orientation on mechanical properties and dimensional accuracy of 3D printed porous samples for bone tissue engineering. *PLoS One*. 2014;9(9):e108252.
21. Yao Q, Wei B, Guo Y, Jin C, Du X, Yan C, et al. Design, construction and mechanical testing of digital 3D anatomical data-based PCL–HA bone tissue engineering scaffold. *J Mater Sci Mater Med*. 2015;26(1):1–9.
 22. Cox SC, Thornby JA, Gibbons GJ, Williams MA, Mallick KK. 3D printing of porous hydroxyapatite scaffolds intended for use in bone tissue engineering applications. *Mater Sci Eng C*. 2015;47:237–47.
 23. Hollister SJ, Flanagan CL, Zopf DA, Morrison RJ, Nasser H, Patel JJ, et al. Design control for clinical translation of 3D printed modular scaffolds. *Ann Biomed Eng*. 2015;43(3):774–86.
 24. Luo Y, Zhai D, Huan Z, Zhu H, Xia L, Chang J, et al. Three-dimensional printing of hollow-struts-packed bioceramic scaffolds for bone regeneration. *ACS Appl Mater Interfaces*. 2015;7(43):24377–83.
 25. Brunello G, Sivoletta S, Meneghello R, Ferroni L, Gardin C, Piattelli A, et al. Powder-based 3D printing for bone tissue engineering. *Biotechnol Adv*. 2016;34(5):740–53.
 26. Xinning Y, Jinghua F, Jianyang L, Xianyan Y, Dongshuang H, Zhongru G, et al. [Fabrication of bioactive tissue engineering scaffold for reconstructing calcified cartilage layer based on three-dimension printing technique]. *Zhejiang da xue xue bao Yi xue ban= Journal of Zhejiang University Medical Sciences*. 2016;45(2):126–31.
 27. Cooke MN, Fisher JP, Dean D, Rinnac C, Mikos AG. Use of stereolithography to manufacture critical-sized 3D biodegradable scaffolds for bone ingrowth. *J Biomed Mater Res B Appl Biomater*. 2003;64(2):65–9.
 28. Gonçalves EM, Oliveira FJ, Silva RF, Neto MA, Fernandes MH, Amaral M, et al. Three-dimensional printed PCL-hydroxyapatite scaffolds filled with CNTs for bone cell growth stimulation. *J Biomed Mater Res B Appl Biomater*. 2016;104(6):1210–9.
 29. Provaggi E, Leong JJ, Kalaskar DM. Applications of 3D printing in the management of severe spinal conditions. *Proc Inst Mech Eng H J Eng Med*. 2017;231(6):471–86.
 30. Moore WR, Graves SE, Bain GI. Synthetic bone graft substitutes. *ANZ J Surg*. 2001;71(6):354–61.
 31. Costa MA, Barbosa A, Neto E, Sa-e-Sousa A, Freitas R, Neves JM, et al. On the role of subtype selective adenosine receptor agonists during proliferation and osteogenic differentiation of human primary bone marrow stromal cells. *J Cell Physiol*. 2011;226(5):1353–66.
 32. Mediero A, Frenkel SR, Wilder T, He W, Mazumder A, Cronstein BN. Adenosine A2A receptor activation prevents wear particle-induced osteolysis. *Sci Transl Med*. 2012;4(135):135ra65.
 33. Mediero A, Cronstein BN. Adenosine and bone metabolism. *Trends Endocrinol Metab*. 2013;24(6):290–300.
 34. Mediero A, Wilder T, Perez-Aso M, Cronstein BN. Direct or indirect stimulation of adenosine A2A receptors enhances bone regeneration as well as bone morphogenetic protein-2. *FASEB J*. 2015;29(4):1577–90.
 35. Mediero A, Wilder T, Reddy VS, Cheng Q, Tovar N, Coelho PG, et al. Ticagrelor regulates osteoblast and osteoclast function and promotes bone formation in vivo via an adenosine-dependent mechanism. *FASEB J*. 2016;30(11):3887–900.
 36. Martin C, Leone M, Viviani X, Ayem ML. High adenosine plasma concentration as a prognostic index for outcome in patients with septic shock. *Crit Care*. 2000;28(9):3198–202.
 37. Cronstein BN, Kramer SB, Weissmann G, Hirschhorn R. A new physiological function for adenosine: regulation of superoxide anion production. *Trans Assoc Am Phys*. 1983;96:384–91.
 38. Haskó G, Cronstein BN. Adenosine: an endogenous regulator of innate immunity. *Trends Immunol*. 2004;25(1):33–9.
 39. Haskó G, Pacher P, Deitch EA, Vizi SE. Shaping of monocyte and macrophage function by adenosine receptors. *Pharmacol Ther*. 2007;113(2):264–75.
 40. Evans BAJ, Elford C, Pexa A, Francis K, Hughes AC, Deussen A, et al. Human osteoblast precursors produce extracellular adenosine, which modulates their secretion of IL-6 and osteoprotegerin. *J Bone Miner Res*. 2006;21(2):228–36.
 41. Kara FM, Doty SB, Boskey A, Goldring S, Zaidi M, Fredholm BB, et al. Adenosine A1 receptors regulate bone resorption in mice: adenosine A1 receptor blockade or deletion increases bone density and prevents ovariectomy-induced bone loss in adenosine A1 receptor-knockout mice. *Arthritis Rheum*. 2010;62(2):534–41.
 42. Mediero A, Kara FM, Wilder T, Cronstein BN. Adenosine A(2A) receptor ligation inhibits osteoclast formation. *Am J Pathol*. 2012;180(2):775–86.
 43. Mediero A, Wilder T, Perez-Aso M, Cronstein BN. Direct or indirect stimulation of adenosine A2A receptors enhances bone regeneration as well as bone morphogenetic protein-2. *FASEB Journal*. 2015;29(4):1577–90.
 44. Gharibi B, Abraham AA, Ham J. Adenosine receptor subtype expression and activation influence the differentiation of mesenchymal stem cells to osteoblasts and adipocytes. *J Bone Miner Res*. 2011;26(9):2112–24.
 45. Costa AM, Barbosa A, Neto E, Sousa SA, Freitas R, Neves JM, et al. On the role of subtype selective adenosine receptor agonists during proliferation and osteogenic differentiation of human primary bone marrow stromal cells. *J Cell Physiol*. 2011;226(5):1353–66.
 46. Rath-Wolfson L, Bar-Yehuda S, Madi L, Ochaion A, Cohen S, Zabutti A, et al. IB-MECA, an A3 adenosine receptor agonist prevents bone resorption in rats with adjuvant induced arthritis. *Clin Exp Rheumatol*. 2006;24(4):400–6.
 47. FitzGerald GA. Dipyridamole. *N Engl J Med*. 1987;316(20):1247–57.

48. Patrono C, Collier B, Dalen JE, Fuster V, Gent M, Harker LA, et al. Platelet-active drugs: the relationships among dose, effectiveness, and side effects. *Chest*. 1998;114(5 Suppl):234S–64S.
49. Monagle P, Chan AKCKC, Goldenberg NA, Ichord RN, Journeycake JM, Nowak-Göttl U, et al. Antithrombotic therapy in neonates and children: Antithrombotic Therapy and Prevention of Thrombosis, 9th ed: American College of Chest Physicians Evidence-Based Clinical Practice Guidelines. *Chest*. 2012;141(2 Suppl):e737S–801S.
50. Ishack S, Mediero A, Wilder T, Ricci JL, Cronstein BN. Bone regeneration in critical bone defects using three-dimensionally printed β -tricalcium phosphate/hydroxyapatite scaffolds is enhanced by coating scaffolds with either dipyridamole or BMP-2. *J Biomed Mater Res B Appl Biomater*. 2017;105(2):366–75.
51. Slater BJ, Kwan MD, Gupta DM, Lee JK, Longaker MT. The role of regional posterior frontal dura mater in the overlying suture morphology. *Plast Reconstr Surg*. 2009;123(2):463–9.
52. Coelho PG, Jimbo R, Tovar N, Bonfante EA. Osseointegration: hierarchical designing encompassing the micrometer, micrometer, and nanometer length scales. *Dent Mater*. 2015;31(1):37–52.
53. Weinand C, Neville CM, Weinberg E, Tabata Y, Vacanti JP. Optimizing biomaterials for tissue engineering human bone using mesenchymal stem cells. *Plast Reconstr Surg*. 2016;137(3):854–63.
54. Cooper GM, Miller ED, DeCesare GE, Usas A, Lensie EL, Bykowski MR, et al. Inkjet-based biopatterning of bone morphogenetic protein-2 to spatially control calvarial bone formation. *Tissue Eng Part A*. 2010;16(5):1749–59.